Humanoid Robot Gait Generation Based on Limit Cycle Stability

Mingguo Zhao, Ji Zhang, Hao Dong,
Yu Liu, Liguo Li, and Xuemin Su

Department of Automation
Tsinghua University, Beijing, P.R. China
mgzhao@mail.tsinghua.edu.cn,
{ji-zhang03,donghao00,liuyu,
lilg06,suxm06}@mails.thu.edu.cn
www.au.tsinghua.edu.cn/robotlab/rwg

Abstract. This paper presents the gait generation and mechanical design of a humanoid robot based on a limit cycle walking method- *Virtual Slope Control*. This method is inspired by Passive Dynamic Walking. By shortening the swing leg, the robot walking on level ground can be considered as on a virtual slope. Parallel double crank mechanisms and elastic feet are introduced to the 5 DoF robot leg, to make the heelstrike of the swing leg equivalent to the point-foot collision used in *Virtual Slope Control*. In practical walking, the gait is generated by connecting the two key frames in the sagittal and lateral plane with sinusoids. With the addition of leg rotational movement, the robot achieves a fast forward walking of 2.0leg/s and accomplishes omnidirectional walking favorably.

1 Introduction

Zero-Moment Point is a well known method wildly used on humanoid robots [1,2,3,4] including Asimo [5], HRP [6], and Qrio [7]. In the RoboCup Humanoid League, there is the leading team Darmstadt Dribblers [8,9] etc. In ZMP walking, stability is ensured by constraining the stance foot to remain in flat contact with the ground at all times [10]. Such an artificial constraint is somewhat too restrictive in that it inherently limits the performance of the gait [11]. The robots are under-achieving in terms of speed, efficiency, disturbance handling, and natural appearance compared to human walking [12].

Limit Cycle Walking is a new conception for biped walking, where the periodic sequence of the steps is stable as a whole but not locally stable at every instant in time [13]. Compared with ZMP, Limit Cycle Walking has fewer artificial constraints and more freedom for finding efficient, fast and robust walking motions [11]. One typical paradigm of Limit Cycle Walking is Passive Dynamic Walking, which presents human-like natural motions when the robot walks on a shallow slope without any actuation, powered only by gravity [14,15,16,17]. Among the existing 2D and 3D robots with active joints, Limit Cycle Walking and Passive

L. Iocchi et al. (Eds.): RoboCup 2008, LNAI 5399, pp. 403–413, 2009.

Dynamic based robots have more advantages in terms of energy efficiency and disturbance rejection ability [12,18,19,20,21].

To realize Passive Dynamic based powered walking on level ground, our idea is to create a virtual slope for the robot by bending the knee of the swing leg and extending the knee of the stance leg. For a fixed gait, only three conditions are needed to keep the walking stable, all of which are easily satisfied. Therefore such a method could become predominant for real-time applications such as the RoboCup humanoid competition. We name this powered walking method *Virtual Slope Control*.

According to the principle of *Virtual Slope Control*, a humanoid robot Stepper_3D was designed using parallel double crank mechanisms and elastic feet. For practical walking, we designed a simple gait, which has only two key frames in the sagittal plane. The gait has eight parameters, all of which have strongly intuitive meanings that make parameters tuning effortless. With only a few hours of hand tuning, the robot presented good walking results.

The remainder of this paper is organized as follows. In Section 2, the *Virtual Slope Control* method is introduced. In Section 3, the mechanical design of our humanoid robot Stepper_3D is presented. In Section 4, we illustrate the gait for practical walking. Section 5 presents the experiment results and Section 6 the conclusion and future work.

2 Virtual Slope Control Method

2.1 Principium of Virtual Slope Control

In Passive Dynamic Walking, a robot walks along a down hill slope without any actuation, as shown in Fig. 1, the gravity potential energy provided by the slope turns into walking kinetic energy and gets lost at heelstrike [14]. If the slope inclination angle is appropriate, the complementary gravity potential energy E_s equals the heelstrike releasing energy E_r and a stable gait can be synthesized [16].

In level walking, our idea is to make the robot walk as on a virtual slope. As shown in Fig. 2, we suppose that the robot leg length can be infinitely shortened. During each walking step, the swing leg is shortened by a fixed ratio. In this way, the body of the robot experiences a virtual slope. As in Passive Dynamic Walking, if the inclination angle of the virtual slope is appropriate, a stable gait could be synthesized.

In practical walking, the leg length of the robot can not be infinitely shortened, so in the swing phase, we actively extend the stance leg that has been shortened in the last walking step (Fig. 3). The leg shortening and extending is actualized by bending and unbending the knee joint. When extending the stance leg, an amount of energy E_c is added into the walking system. If this energy equals the gravity potential energy provided by the virtual slope E_s and the heelstrike releasing energy E_r (Fig. 4), a stable gait can be synthesized on level ground.

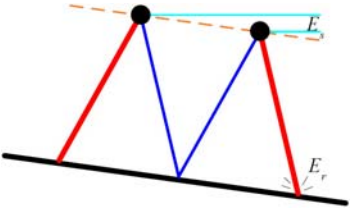

Fig. 1. Passive Dynamic Walking

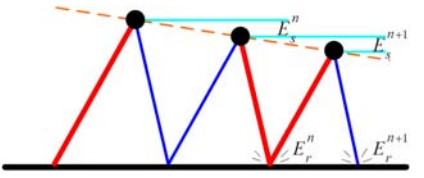

Fig. 2. Virtual Slope Walking by Shortening Legs

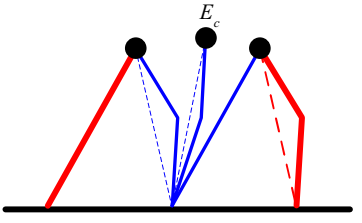

Fig. 3. Actively Extending the Stance Leg and Complementary Energy E_c

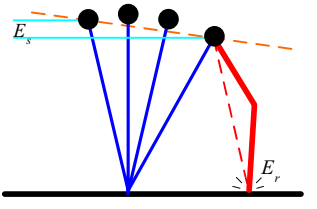

Fig. 4. Gravity Potential Energy Provided by Virtual Slope E_s and Heelstrike Releasing Energy E_r

2.2 Basic Conditions for Powered Stable Walking with Virtual Slope Control

The theoretical analysis of the *Virtual Slope Control* method is based on the model of two massless legs and a point mass trunk. For a fixed robot gait, whose joint angular velocities at heelstrike are zero, only the three following conditions have to be satisfied for stable walking.

(1) The angular velocity of the stance leg should be a small positive value, otherwise the stance leg would leave the ground by the pulling of centrifugal force. In the following inequation, θ/T is the mean of the angular velocity of the stance leg in one waking step; α_0 is the initial angle of the stance leg (Fig. 5); θ is the angle between the two legs at heelstrike; T is the walking period; r is the

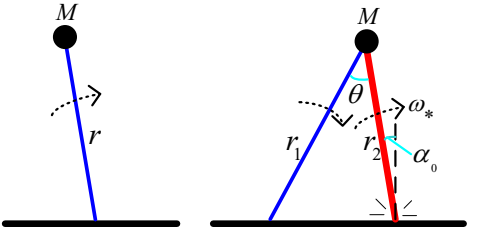

Fig. 5. Variables used in Basic Walking Conditions, Left: Swing; Right: Heelstrike

length of the stance leg; r_1 is the length of the swing leg right after heelstrike; r_2 is the length of the stance leg right after heelstrike; And g is the acceleration of gravity.

$$0 < \frac{\theta}{T} \leq \sqrt{(g\cos(\theta - \alpha_0) + \min r'')/r_1} \tag{1}$$

(2) The complementary energy provided by extending the stance leg should be equal to the heelstrike releasing energy, while E_c is the complementary energy; E_r is the heelstrike releasing energy; M is the mass of the trunk (Fig. 5); ω_* is the angular velocity of the stance leg right after heelstrike; And t is the time variable.

$$\begin{aligned} E_c &= \int_0^T Mg\cos(\alpha_0 - \tfrac{\theta}{T}t)r'\mathrm{d}t - \tfrac{1}{2}M\tfrac{\theta}{T^2}{}^2(r_1^2 - r_2^2) \\ &= E_r = \tfrac{1}{2}Mr_2^2\omega_*^2\tan^2\theta \end{aligned} \tag{2}$$

(3) The gait should be robust to small disturbances. The stability of the gait is analyzed with the Poincaré map at the beginning of one step. Assuming linear behavior, the relation between the perturbations of step n and step $n+1$ is $[\Delta\omega_{n+1}\Delta t_{n+1}]^T = J\,[\Delta\omega_n\Delta t_n]^T$. For a stable gait, the eigenvalues λ of the Jacobi matrix J should be within the unit circle in the complex plane. Therefore the following equation should be satisfied. From such equation, it is also indicated that extending the stance leg late could enhance walking stability.

$$\int_0^T \sin(\alpha_0 - \frac{\theta}{T}t)r'\mathrm{d}t < 0 \quad r' \geq 0 \tag{3}$$

3 Mechanism of Stepper_3D

3.1 Overall Introduction

Stepper_3D (Fig. 6) is the lower body of the humanoid robot which will be used in RoboCup 2008 by the Tsinghua Hephaestus team. Its structure is designed under the competition rules of the RoboCup Humanoid League [22]. The robot is 0.44m in height and 2.51kg in weight. Dimensional parameters are shown in Fig. 7. The robot has 11 DoF: 1 yaw DoF on top of the trunk, 3 orthogonal DoF at each hip, 1 pitch DoF at each knee, and 1 roll DoF at each ankle. All the DoF are actuated by Robotis digital servo motors.

The uniqueness of Stepper_3D comes from adopting the parallel double crank leg mechanism shown in Fig. 6. This design arises from the principle of *Virtual Slope Control*, and its foundation-Limit Cycle Walking, where the state of the robot at heelstrike is significant, while the exact trajectory in the swing phase is less relevant [11]. By adopting the parallel double crank mechanisms, we are able to mechanically constrain the feet to be parallel to the ground at heelstrike, and avoid the angular cumulative errors caused by the joint motors in normally designed legs. Therefore, the flat foot at heelstrike can be approximated by the point-foot model as in *Virtual Slope Control*. Additionally, this design saves the two ankles' pitch DoF and reduces the weight of the legs. The mass distribution of the robot is closer to the theoretical model of two massless legs and a mass point trunk (Fig. 5).

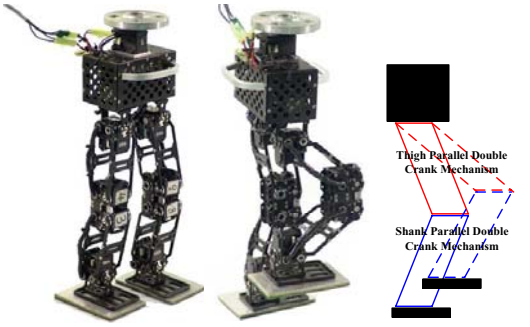

Fig. 6. Stepper_3D with the parallel double crank leg mechanism

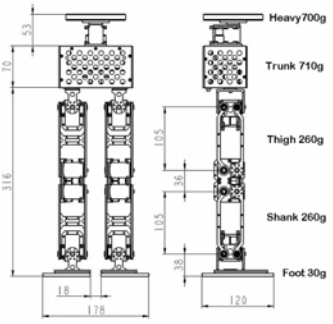

Fig. 7. Stepper_3D Structure and Body Parameters

3.2 Details of Mechanism Design

The leg of Stepper_3D is composed of two sets of parallel double crank mechanisms (Fig. 6), forming the thigh and shank respectively. Since this mechanism has only one DoF, any of the four vertexes can be used as the active rotating axis, while the other three rotate passively. On Stepper_3D, the active rotating axes are placed at the front vertexes of the knee joint (Fig. 8), while the hip and ankle vertexes act as passive ones (Figs. 9, 10).

During the swing phase, there might be a slight angle between the sole of the stance leg and the ground. To reduce its impact on the walking stability, we used flexible materials on the bottom of the feet. As shown in Fig. 10, the soft sponge cushion is added under the elastic aluminum sheet which is placed under the rigid baseboard.

The batteries and processing boards are all located inside the trunk box (Fig. 11) rather than on the legs or feet, decreasing the mass of the legs to better approach the theoretical model. An iron weight approximating the upper body's mass and inertia is placed above the trunk (Fig. 11) to simulate the completed robot walking conditions.

Fig. 8. Knee

Fig. 9. Hip

Fig. 10. Ankle

Fig. 11. Trunk

4 Virtual Slope Control for Practical Walking

4.1 Movement in the Sagittal Plane

As shown in Fig. 12, in each walking step, the robot bends its swing leg, and extends its stance leg to restore the walking energy. Since the feet are mechanically constrained to be parallel to the trunk in the sagittal plane, the gait in the sagittal plan equals that of a point-foot robot. Since *Virtual Slope Control* is based on Limit Cycle Stability [11], the sticking point is the state of the heelstrike, so we put a Heelstrike Key Frame therein. To prevent the swing leg from dragging on the ground, we placed a Swing Key Frame at the midpoint of the swing phase. The two key frames are described by four parameters as in Fig. 12. Since the exact trajectories of the joint angles are of little concern in limit cycle walking [11], we simply use smooth sinusoids to connect the key frames as described by Eq. 4 and Eq. 5. The connected trajectories are shown in Fig. 14 and the definitions of the joint angles are shown in Fig. 13.

In the four gait parameters shown in Fig. 12, θ is related to the step length. In practical walking, it is equally divided between the two hip joints. α is related to the complementary energy, the larger α is, the more walking energy is complemented. β is related to the lifting height of the swing leg, and T is the step period. It is intuitive that a walk with a higher step frequency (small T) or

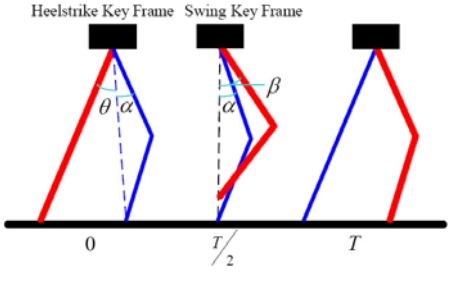

Fig. 12. Sagittal Movement

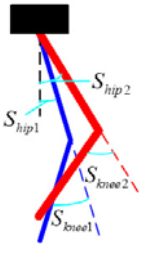

Fig. 13. Definitions of Joint Angles in Sagittal Plane

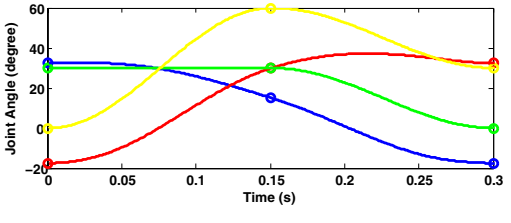

Fig. 14. Trajectories of Sagittal Joint Angles in One Walking Step. $T = 0.3s, \theta = 35^\circ, \alpha = 15^\circ, \beta = 30^\circ$, The cycles denote the key frames. Blue: Hip1; Red: Hip2; Green: Knee1; Yellow: Knee2.

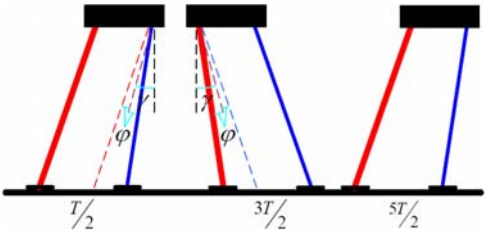

Fig. 15. Lateral Swing Movement

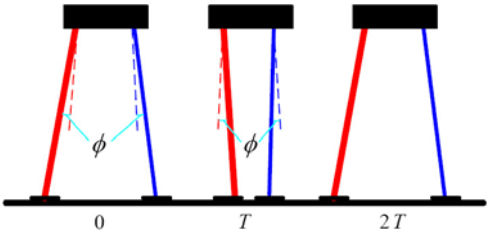

Fig. 16. Lateral Step Movement

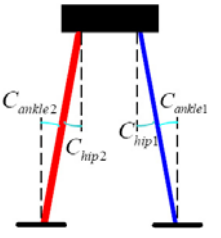

Fig. 17. Definitions of Joint Angles in Lateral Plane

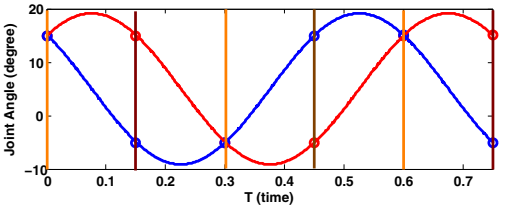

Fig. 18. Trajectories of Lateral Joint Angles in 2.5 Walking Steps. $T = 0.3s, \varphi = 5^\circ, \gamma = 10^\circ, \phi = 10^\circ$; Blue: Hip1, Ankle1; Red: Hip2, Ankle2;Brown: Lateral Swing Key Frames; Orange: Lateral Step Key Frames.

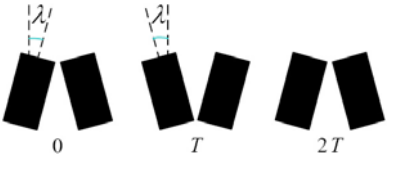

Fig. 19. Rotational Movement

a larger step length (large θ) costs more energy. So the faster the walking is, the larger α should be. Let $\theta = 0, \alpha = 0$, the robot march in place.

This gait can easily satisfy the three basic walking conditions. First by giving a bigger T and a smaller θ, condition (1) can be satisfied. Second, by changing α, the complementary energy can be adjusted to satisfy condition (2). Finally, the

robot stance leg is extended between the Swing Key Frame and the Heelstrike Key Frame, which is in the second half of the walking step, thus condition (3) can be satisfied.

$$\begin{cases} S_{hip1} = \frac{\theta}{2}\cos\frac{\pi t}{T} + \alpha \\ S_{hip2} = -\frac{\theta}{2}\cos\frac{\pi t}{T} + \frac{\beta}{2}(1-\cos\frac{2\pi t}{T}) \\ S_{knee1} = 2\alpha \\ S_{knee2} = \beta(1-\cos\frac{2\pi t}{T}) \end{cases} 0 < t \leq T/2 \tag{4}$$

$$\begin{cases} S_{hip1} = \frac{\theta}{2}\cos\frac{\pi t}{T} + \frac{\alpha}{2}(1-\cos\frac{2\pi t}{T}) \\ S_{hip2} = -\frac{\theta}{2}\cos\frac{\pi t}{T} + \alpha + \frac{\beta-\alpha}{2}(1-\cos\frac{2\pi t}{T}) \\ S_{knee1} = \alpha(1-\cos\frac{2\pi t}{T}) \\ S_{knee2} = 2\alpha + (\beta-\alpha)(1-\cos\frac{2\pi t}{T}) \end{cases} T/2 < t \leq T \tag{5}$$

4.2 Movement in the Lateral Plane

In the lateral plane, we define two movements: Lateral Swing Movement (Fig. 15) and Lateral Step Movement (Fig. 16). The Lateral Swing Movement serves in every gait while the Lateral Step Movement contributes to lateral walking and omnidirectional walking. Each movement includes two key frames. In the key frames shown in Fig. 15, γ indicates the lateral swing amplitude. φ indicates the angle between the two legs and in part determines the lateral swing period [15]. So adjusting φ could synchronize the lateral movement and sagittal movement. In the key frames shown in Fig. 16, ϕ indicates the lateral step length. The feet are controlled to be parallel to the trunk. The key frames are connected by sinusoids as Eq 6. The connected trajectories are shown in Fig. 18 and the definitions of the joint angles are shown in Fig. 17.

$$\begin{cases} C_{hip1} = C_{ankle1} = \varphi - \frac{\gamma}{2}\sin\frac{\pi t}{T} + \phi\cos\frac{\pi t}{T} \\ C_{hip2} = C_{ankle2} = \varphi + \frac{\gamma}{2}\sin\frac{\pi t}{T} + \phi\cos\frac{\pi t}{T} \end{cases} \tag{6}$$

4.3 Rotational Movement

To the rotational movement, we put two key frames as in Fig. 19 and use sinusoids for the connection, while λ indicates the rotation amplitude.

5 Experiment Results

5.1 Forward Walking

By tuning the four parameters of the sagittal movement θ, α, β, T (Fig. 12) and the two parameters of the lateral swing movement φ, γ (Fig. 15), Stepper_3D presented a fast and stable walking and reached the speed of 0.5m/s and the relative speed of 2.0leg/s. By giving different θ and α, the robot could change its speed continuously from 0m/s to 50cm/s. The video frames of forward walking are shown in Fig. 20. The comparison of our result to those of the other robots in RoboCup 2008 is shown in Fig. 23.

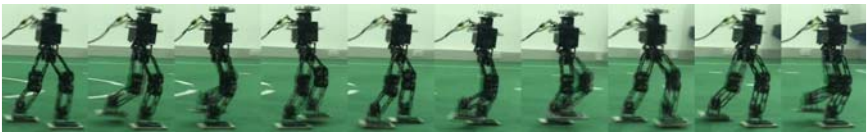

Fig. 20. Forward Walking Video Frames

Fig. 21. Lateral Walking Video Frames

Fig. 22. Rotation Video Frames

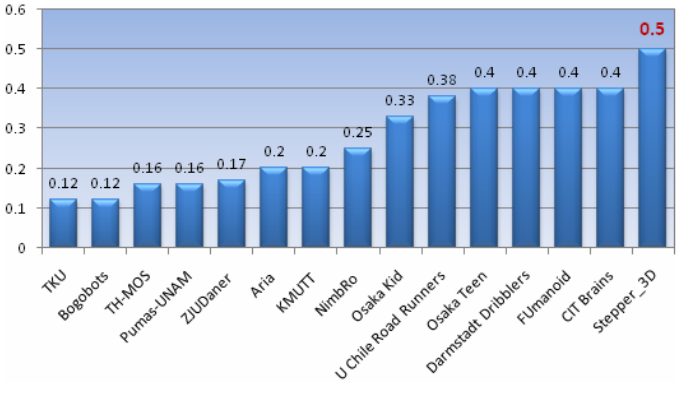

Fig. 23. Comparison of Walking Speed (m/s). All the robots on RoboCup 2008 whose speed exceed 0.1m/s are presented in the figure. Stepper_3D reached the speed of 0.5m/s.

5.2 Lateral Walking and Rotation

By setting $\theta = 0, \alpha = 0$, tuning β, T (Fig. 12) and φ, γ (Fig. 15), the robot could march in place. Then by giving a slight value to the lateral step parameter ϕ (Fig. 16) or rotation parameter λ (Fig. 19), it could walk sideward or rotate as shown in Figs. 21, 22.

5.3 Omnidirectional Walking

While lateral walking and rotation could be realized by adding the lateral step movement and rotation movement to the gait of marching in place respectively, omnidirectional walking can be realized by adding the two movements to forward walking. In this way, Stepper_3D accomplished walking and rotating simultaneously. All the videos about the walking experiments could be found on our website http://www.au.tsinghua.edu.cn/robotlab/rwg/Robots.htm.

6 Conclusion and Future Work

In this paper, we present the mechanical design and gait generation of our humanoid robot Stepper_3D based on a limit cycle walking method-*Virtual Slope Control*. The parallel double crank mechanism is adopted and the elastic materials are used on the bottom of the feet. The gait is extraordinarily simple with strongly intuitive parameters, which results in a very high walking speed and also accomplishes omnidirectional walking favorably. The experiment results indicate that the mechanical design and the gait of *Virtual Slope Control* are suitable for RoboCup Competitions.

Currently, we are working on the theoretical analysis of energy supplementation and walking stability. Hopefully, such work will start to appear in our papers in two or three months. Since this paper only deals with a fixed gait, other possible avenues for future work involve sensor feedback introduction, gait adjustment, and active gait switching.

Acknowledgments. The authors would like to thank the Tsinghua Hephaestus team. This work was supported in part by the Open Project Foundation of National Industrial Control Technology Key Lab (No. 0708003) and Open Project Foundation of National Robotics Technology and System Key Lab of China(No. SKLRS200718).

References

1. Vukobratovic, M., Juricic, D.: Contribution to the synthesis of biped gait. In: Proc. IFAC Symp. Technical and Biological Problem on Control, Erevan, USSR (1968)
2. Juricic, D., Vukobratovic, M.: Mathematical Modeling of Biped Walking Systems (ASME Publ., 1972) 72-WA/BHF-13 (1972)
3. Vukobratovic, M., Stepanenko, Y.: Mathematical models of general anthropomorphic systems. Mathematical Biosciences 17, 191–242 (1973)
4. Vukobratovic, M.: How to control the artificial anthropomorphic systems. IEEE Trans. System, Man and Cybernetics SMC-3, 497–507 (1973)
5. Hirose, M., Haikawa, Y., Takenaka, T., et al.: Development of humanoid robot ASIMO. In: Proc. IEEE/RSJ International Conference on Intelligent Robots and Systems, Workshop 2, Maui, HI, USA, October 29 (2001)
6. Kaneko, K., Kanehiro, F., Kajita, S., et al.: Humanoid robot HRP-2. In: Proc. IEEE International Conference on Robotics and Automation (ICRA), New Orleans, LA, USA, April 26 - May 1, pp. 1083–1090 (2004)

7. Nagasaka, K., Kuroki, Y., Suzuki, S., et al.: Integrated motion control for walking, jumping and running on a small bipedal entertainment robot. In: Proc. IEEE International Conference on Robotics and Automation (ICRA), New Orleans, LA, USA, April 26 - May 1, vol. 4, pp. 3189–3194 (2004)
8. Friedmann, M., Kiener, J., Petters, S., et al.: Versatile, high-quality motions and behavior control of humanoid soccer robots. In: Proc. 2006 IEEE-RAS International Conference on Humanoid Robots, Genoa, Italy, December 4, pp. 9–16 (2006)
9. Hemker, T., Sakamoto, H., Stelzer, M., et al.: Hardware-in-the-Loop Optimization of the Walking Speed of a Humanoid Robot. In: Proc. CLAWAR 2006, Brussels, Belgium, September 12-14 (2006)
10. Vukobratovic, M., Frank, A., Juricic, D.: On the Stability of Biped Locomotion. IEEE Transactions on Biomedical Engineering 17(1) (1970)
11. Hobbelen, D., Wisse, M.: Limit Cycle Walking. In: Humanoid Robots: Human-like Machines, ch. 14, p. 642. I-Tech Education and Publishing, Vienna (2007)
12. Collins, S., Ruina, A., Tedrake, R., et al.: Efficient Bipedal Passive-Dynamic Walkers. Science 307(5712), 1082–1085 (2005)
13. Hurmuzlu, Y., Moskowitz, G.: Role of Impact in the Stability of Bipedal Locomotion. International Journal of Dynamics and Stability of Systems 1(3), 217–234 (1986)
14. McGeer, T.: Passive Dynamic Walking. International Journal of Robotics Research 9, 62–82 (1990)
15. Garcia, M.: Stability, Scaling, and Chaos in Passive Dynamic Gait Models. PhD Thesis, Cornell University, Ithaca, NY (1999)
16. Wisse, M.: Essentials of Dynamic Walking: Analysis and design of two-legged robots. PhD Thesis, Delft University of Technology, Netherlands (2004)
17. Tedrake, R.: Applied Optimal Control for Dynamically Stable Legged Locomotion. PhD Thesis, MIT, MA (2004)
18. Pratt, J., Chew, C.-M., Torres, A., et al.: Virtual Model Control: An Intuitive Approach for Bipedal Locomotion. The International Journal of Robotics Research 20(2), 129–143 (2001)
19. Chevallereau, C., Abba, G., Aoustin, Y., et al.: RABBIT: a testbed for advanced control theory. IEEE Control Systems Magazine 23(5), 57–79 (2003)
20. Geng, T., Porr, B., Wörgötter, F.: Fast Biped Walking with a Sensor-driven Neuronal Controller and Real-Time Online Learning. The International Journal of Robotics Research 25(3), 243–259 (2006)
21. Morimoto, J., Cheng, G., Atkeson, C.G., et al.: A simple reinforcement learning algorithm for biped walking. In: Proceedings of IEEE International Conference on Robotics and Automation, vol. 3 (2004)
22. Kulvanit, P., Stryk, O.: RoboCup Soccer Humanoid League Rules and Setup for the, competition in Suzhou, China (2008), `https://lists.cc.gatech.edu/mailman/listinfo/robocup-humanoid`